

Speed of sounds bound, tidal polarizability and gravitational waves from neutron stars

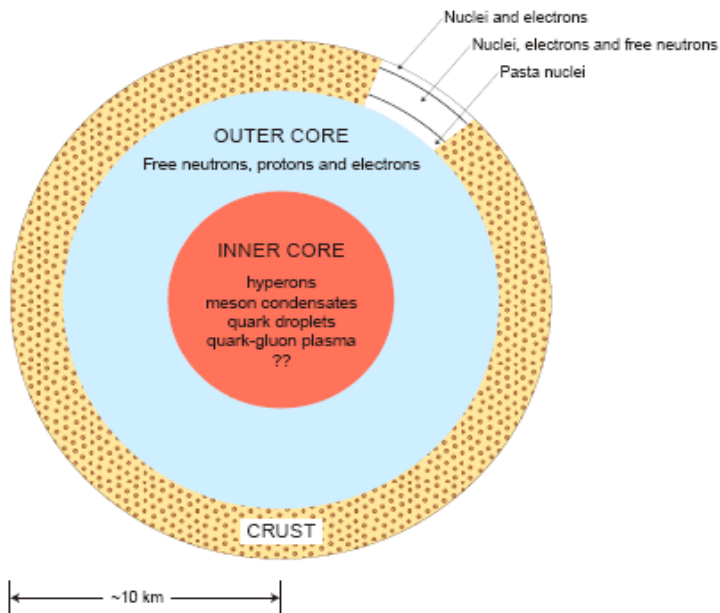
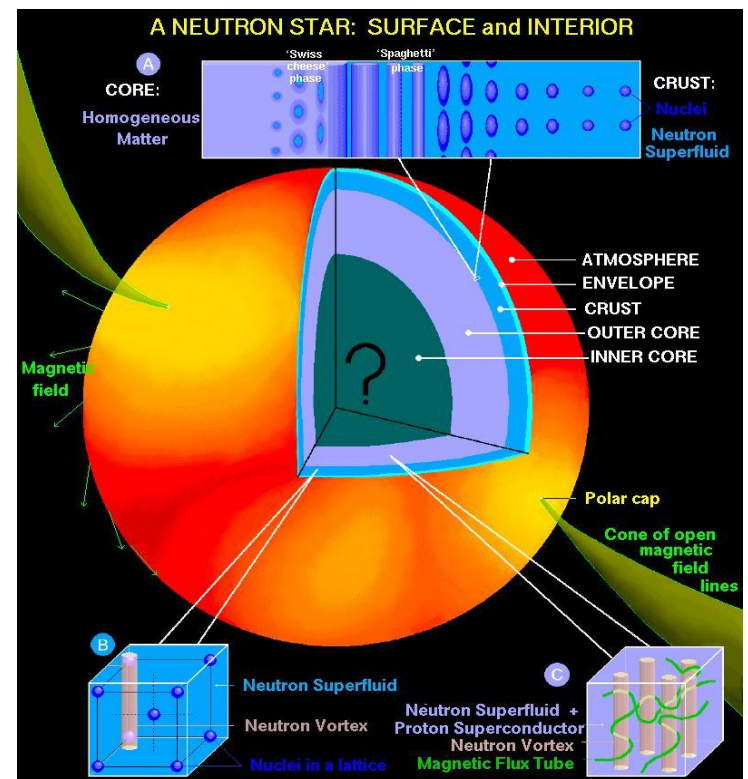
Ch. Moustakidis, T. Gaitanos, C. Margaritis G. Lalazissis
Department of Theoretical Physics,
Aristotle University of Thessaloniki, Greece

4th Workshop on New Aspects and Perspectives in Nuclear Physics (HINPW4)

5-6 May 2017, Ioannina, Greece

Outline

- A. Introduction on neutron star structure and nuclear equation of state**
- B. The speed of sound in nuclear matter and relative constraints.
Implication on the maximum neutron star mass (MNSM)**
- C. Relativistic kinetic theory constraints on MNSM**
- D. Tidal polarizability**
- E. Presentation of the results**
- D. Main conclusions and perspectives**



Properties of Neutron Stars

Radius: $R \sim 10\text{--}15\text{ km}$

Mass: $M \sim 1.4\text{--}2.5\text{ Msolar}$

Mean density: $\rho(r) \sim 4 \times 10^{14}\text{ g/cm}^3$

Frequency: few Hz– 700 Hz

Magnetic field: $B \sim 100\text{--}1000\text{ G}$

The knowledge of maximum neutron star mass is important since:

- 1. Helps to identify a compact object as a black hole.**
- 2. The accurate calculation of MNSM strongly depends on the knowledge of the nuclear equation of state up to very high densities.**
- 3. Related with the appearance of hyperons and other degrees of freedom.**
- 4. Helps to understand some of the more extreme NS related processes like core-collapse supernovae, magnetar flares, and NS mergers.**

The basic assumptions

We consider the assumptions¹

1. the matter of the neutron star is a perfect fluid described by a one-parameter equation of state between the pressure P and the density ρ
2. the density ρ is non negative (due to attractive character of gravitational forces)
3. the matter is microscopically stable, which is ensured by the conditions $P \geq 0$ and $dP/d\rho \geq 0$
4. below a critical density ρ_c the equation of state is well known

From the above assumptions and the TOV equations it follows that the density and pressure decreases outward in the star. In addition the radius R_c at which the pressure is $P_c = P(\rho_c)$ divides the neutron star into two regions. The core where $r \leq R_c$ and $\rho \geq \rho_c$ and the envelope where $r \geq R_c$ and $\rho \leq \rho_c$.

¹C.E. Rhoades Jr. and R. Ruffini, Phys. Rev. Lett. **32**, 324 (1974)

The upper limits of the speed of sound

The speed of sound is defined as

$$\frac{v_s}{c} = \left(\frac{\partial P}{\partial \mathcal{E}} \right)_S^{1/2}$$

We consider the following three limits for the speed of sound

1. $\frac{v_s}{c} \leq 1$: causality limit from special relativity²
2. $\frac{v_s}{c} \leq \frac{1}{\sqrt{3}}$: from QCD and other theories³
3. $\frac{v_s}{c} \leq \left(\frac{\mathcal{E} - P/3}{P + \mathcal{E}} \right)^{1/2}$: from relativistic kinetic theory⁴

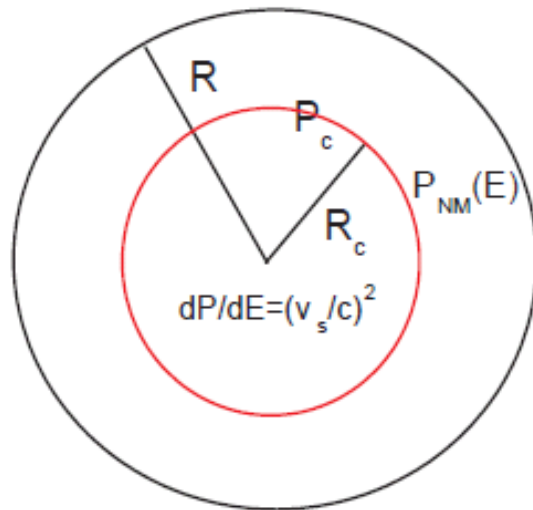
²J.B. Hartle, Phys. Rep. **46**, 201 (1978)

³P. Bedaque and A.W. Steiner, Phys.Rev.Lett. **114**, 031103 (2015).

⁴T.S. Olson, Phys. Rev. C **63**, 015802 (2002)

The maximum mass configuration achieved according to the following structure for the neutron star EoS

$$P(\mathcal{E}) = \begin{cases} P_{crust}(\mathcal{E}), & \mathcal{E} \leq \mathcal{E}_{c-edge} \\ P_{NM}(\mathcal{E}), & \mathcal{E}_{c-edge} \leq \mathcal{E} \leq \mathcal{E}_0 \\ \left(\frac{v_s}{c}\right)^2 (\mathcal{E} - \mathcal{E}_0) + P_{NM}(\mathcal{E}_0), & \mathcal{E}_0 \leq \mathcal{E}. \end{cases}$$



$$v_s = c \sqrt{\frac{\partial P}{\partial \mathcal{E}}}$$

Nuclear equation of state models

The momentum dependent interaction model (Skyrme type)

$$\begin{aligned}
 E_b(n, I) = & \frac{3}{10} E_F^0 u^{2/3} \left[(1+I)^{5/3} + (1-I)^{5/3} \right] + \frac{1}{3} A \left[\frac{3}{2} - \left(\frac{1}{2} + x_0 \right) I^2 \right] u \\
 & + \frac{\frac{2}{3} B \left[\frac{3}{2} - \left(\frac{1}{2} + x_3 \right) I^2 \right] u^\sigma}{1 + \frac{2}{3} B' \left[\frac{3}{2} - \left(\frac{1}{2} + x_3 \right) I^2 \right] u^{\sigma-1}} \\
 & + \frac{3}{2} \sum_{i=1,2} \left[C_i + \frac{C_i - 8Z_i}{5} I \right] \left(\frac{\Lambda_i}{k_F^0} \right)^3 \left(\frac{((1+I)u)^{1/3}}{\frac{\Lambda_i}{k_F^0}} - \tan^{-1} \frac{((1+I)u)^{1/3}}{\frac{\Lambda_i}{k_F^0}} \right) \\
 & + \frac{3}{2} \sum_{i=1,2} \left[C_i - \frac{C_i - 8Z_i}{5} I \right] \left(\frac{\Lambda_i}{k_F^0} \right)^3 \left(\frac{((1-I)u)^{1/3}}{\frac{\Lambda_i}{k_F^0}} - \tan^{-1} \frac{((1-I)u)^{1/3}}{\frac{\Lambda_i}{k_F^0}} \right).
 \end{aligned}$$

The non linear derivative model (NLD)

(Non-linear derivative interactions in relativistic hadrodynamics:

T. Gaitanos, M. Kaskulov and U. Mosel, NPA 828, 9-28 (2009))

$$\mathcal{E} = \sum_{i=p,n} \frac{\kappa}{(2\pi)^3} \int_{|\vec{p}| \leq p_{Fi}} d^3p E(\vec{p}) + \frac{1}{2} \left(m_\sigma^2 \sigma^2 + 2U(\sigma) - m_\omega^2 \omega^2 - m_\rho^2 \rho^2 \right).$$

Microscopic model of neutron matter based on nuclear interaction derived from chiral effective field theory (CEFT): Hebeler et al., PRL, 105 161102 (2010).

$$\frac{E(u, x)}{T_0} = \frac{3}{5} \left[x^{5/3} + (1 - x)^{5/3} \right] (2u)^{2/3} - [(2\alpha - 4\alpha_L)x(1 - x) + \alpha_L] u + [(2\eta - 4\eta_L)x(1 - x) + \eta_L] u^\gamma$$

The H-HJ (Heisenerg and Hjiorth-Jensen) phenomenological model

$$E = E_0 u \frac{u - 2 - d}{1 + du} + S_0 u^\gamma (1 - 2x)^2,$$

The Skyrme model

$$\begin{aligned} E(n, I) = & \frac{3}{10} \frac{\hbar^2 c^2}{m} \left(\frac{3\pi^2}{2} \right)^{2/3} n^{2/3} F_{5/3}(I) + \frac{1}{8} t_0 n [2(x_0 + 2) - (2x_0 + 1)F_2(I)] \\ & + \frac{1}{48} t_3 n^{\sigma+1} [2(x_3 + 2) - (2x_3 + 1)F_2(I)] \\ & + \frac{3}{40} \left(\frac{3\pi^2}{2} \right)^{2/3} n^{5/3} \left[(t_1(x_1 + 2) + t_2(x_2 + 2)) F_{5/3}(I) \right. \\ & \left. + \frac{1}{2} (t_2(2x_2 + 1) - t_1(2x_1 + 1)) F_{8/3}(I) \right], \end{aligned}$$

Relativistic kinetic theory constraints

$$\mathcal{E} \geq 0, \quad P \geq 0, \quad (P + \mathcal{E}) \left(\frac{v_s}{c} \right)^2 \geq 0, \quad \left(\frac{v_s}{c} \right)^2 \leq \frac{\mathcal{E} - P/3}{P + \mathcal{E}}, \quad P \leq 3\mathcal{E}$$

The maximally incompressible EOS is taken from the equality

$$\left(\frac{v_s}{c} \right)^2 = \frac{\mathcal{E} - P/3}{P + \mathcal{E}} \quad n^2 \frac{d^2 \mathcal{E}}{dn^2} + \frac{n}{3} \frac{d\mathcal{E}}{dn} - \frac{4}{3} \mathcal{E} = 0$$

$$\mathcal{E}(n) = \mathcal{C}_1 n^{a_1} + \mathcal{C}_2 n^{a_2} \quad P(n) = \mathcal{C}_1 n^{a_1} (a_1 - 1) + \mathcal{C}_2 n^{a_2} (a_2 - 1),$$

$$\mathcal{C}_1 = \left(\frac{(2 + \sqrt{13})\mathcal{E}(n) + 3P(n)}{2\sqrt{13}} \right) n^{-\frac{1}{3}(1+\sqrt{13})}$$

$$\mathcal{C}_2 = - \left(\frac{(2 - \sqrt{13})\mathcal{E}(n) + 3P(n)}{2\sqrt{13}} \right) n^{-\frac{1}{3}(1-\sqrt{13})}$$

$$P(n) = \begin{cases} P_{crust}(n), & n \leq n_{c-edge} \\ P_{NM}(n), & n_{c-edge} \leq n \leq n_0 \\ \mathcal{C}_1 n^{a_1} (a_1 - 1) + \mathcal{C}_2 n^{a_2} (a_2 - 1), & n_0 \leq n. \end{cases}$$

The values of the constants \mathcal{C}_1 and \mathcal{C}_2 are determined by the help of the matching density n_c .

The TOV Equations

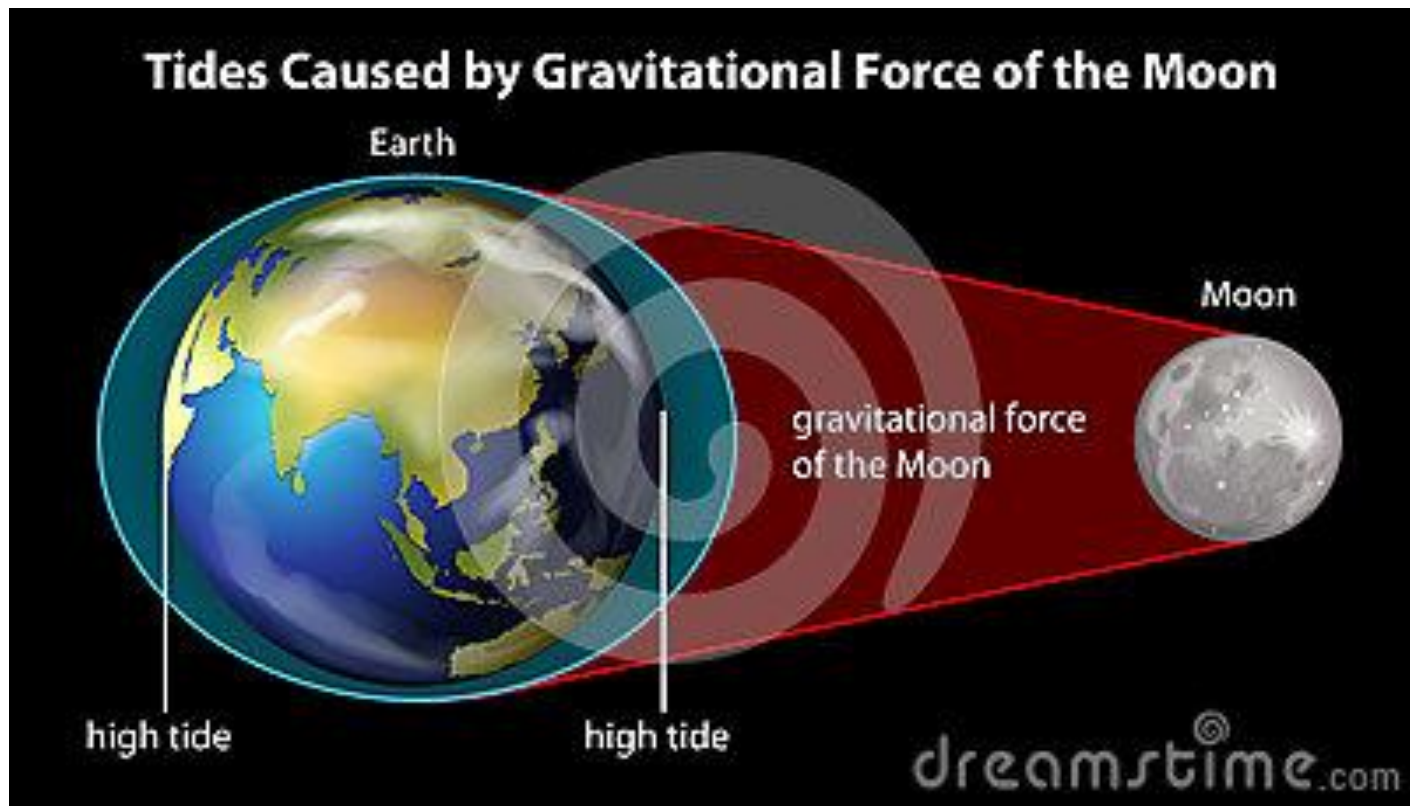
$$\frac{dP(r)}{dr} = -\frac{G\rho(r)M(r)}{r^2} \left(1 + \frac{P}{\rho c^2}\right) \left(1 + \frac{4\pi P(r)r^3}{M(r)c^2}\right) \left(1 - \frac{2GM(r)}{c^2 r}\right)^{-1}$$

$$\frac{dM(r)}{dr} = 4\pi r^2 \rho(r)$$

$$\mathcal{E} = n \left(E + mc^2 \right) = \rho c^2 \quad P = n \frac{d\mathcal{E}}{dn} - \mathcal{E}$$

To solve the TOV equations for $P(r)$ and $M(r)$ one can integrate outwards from the origin ($r = 0$) to the point $r = R$ where the pressure becomes zero. This point defines R as the coordinate radius of the star. To do this, one needs an initial value of the pressure at $r = 0$, called $P_c = P(r = 0)$. The radius R and the total mass of the star, $M \equiv M(R)$, depend on the value of P_c . To be able to perform the integration, one also needs to know the energy density $\mathcal{E}(r)$ (or the density mass $\rho(r)$) in terms of the pressure $P(r)$. This relationship is the equation of state for neutron star matter.

Tidal effects in binary systems



Tidal Polarizability

Gravitational waves from the final stages of in-spiraling binary neutron stars are expected to sources for ground-based gravitational wave detectors

The tidal polarizability and relative effects are potentially measurable when the waveform of the GW is clean

$$Q_{ij} = -k_2 \frac{2R^5}{3G} E_{ij} \equiv -\lambda E_{ij},$$

$$\lambda = 2R^5 k_2 / 3G$$

$$\begin{aligned} k_2 = & \frac{8\beta^5}{5} (1 - 2\beta)^2 [2 - y_R + (y_R - 1)2\beta] \\ & \times \left[2\beta (6 - 3y_R + 3\beta(5y_R - 8)) \right. \\ & + 4\beta^3 (13 - 11y_R + \beta(3y_R - 2) + 2\beta^2(1 + y_R)) \\ & \left. + 3(1 - 2\beta)^2 [2 - y_R + 2\beta(y_R - 1)] \ln(1 - 2\beta) \right]^{-1}, \end{aligned}$$

$$r \frac{dy(r)}{dr} + y^2(r) + y(r)F(r) + r^2 Q(r) = 0, \quad y(0) = 2, \quad y_R \equiv y(R)$$

$$F(r) = \left[1 - \frac{4\pi r^2 G}{c^4} (\mathcal{E}(r) - P(r)) \right] \left(1 - \frac{2M(r)G}{rc^2} \right)^{-1},$$

$$\begin{aligned} r^2 Q(r) = & \frac{4\pi r^2 G}{c^4} \left[5\mathcal{E}(r) + 9P(r) + \frac{\mathcal{E}(r) + P(r)}{\partial P(r)/\partial \mathcal{E}(r)} \right] \left(1 - \frac{2M(r)G}{rc^2} \right)^{-1} \\ & - 6 \left(1 - \frac{2M(r)G}{rc^2} \right)^{-1} \\ & - \frac{4M^2(r)G^2}{r^2 c^4} \left(1 + \frac{4\pi r^3 P(r)}{M(r)c^2} \right)^2 \left(1 - \frac{2M(r)G}{rc^2} \right)^{-2}. \end{aligned}$$

Averaged tidal polarizability for binary neutron star system

$$\tilde{\lambda} = \frac{1}{26} \left[\frac{m_1 + 12m_2}{m_1} \lambda_1 + \frac{m_2 + 12m_1}{m_2} \lambda_2 \right] \quad \begin{array}{l} \lambda_1 = \lambda_1(m_1) \text{ and } \lambda_2 = \lambda_2(m_2) \\ M = m_1 + m_2 \end{array}$$

The dependence on the asymmetry parameter and chirp mass

$$\tilde{\lambda} = \frac{1}{26} \left[\left(1 + 12 \frac{1 - \sqrt{1 - 4h}}{1 + \sqrt{1 + 4h}} \right) \lambda_1(\mathcal{M}, h) + \left(1 + 12 \frac{1 + \sqrt{1 - 4h}}{1 - \sqrt{1 + 4h}} \right) \lambda_2(\mathcal{M}, h) \right].$$

$$\mathcal{M} = (m_1 m_2)^{3/5} / M^{1/5} \quad h = m_1 m_2 / M^2$$

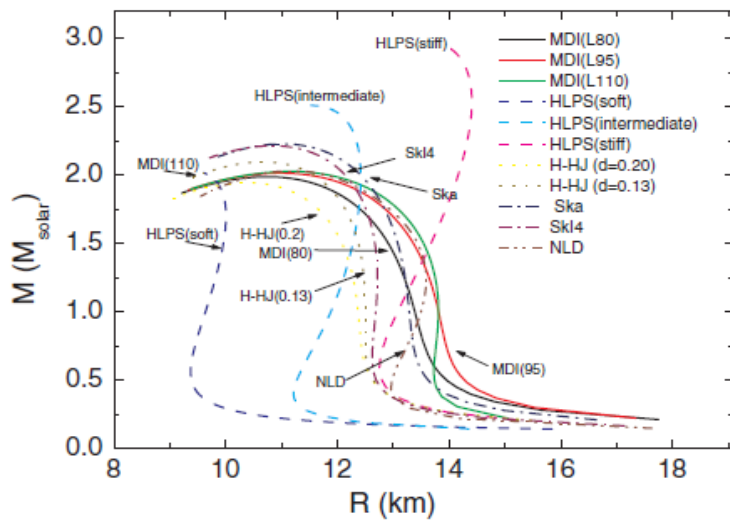


FIG. 1. Mass-radius diagram for the equations of state used in the present work.

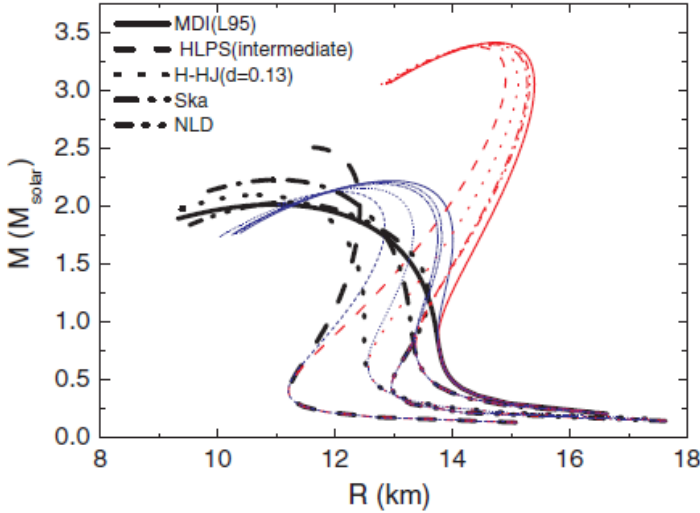


FIG. 3. The mass-radius diagram for five EoSs (EoS/normal case, line with thick width) in comparison with the corresponding maximum mass configuration results of the EoS/minstiff case (line with medium width) and EoS/maxstiff case (line with thin width).

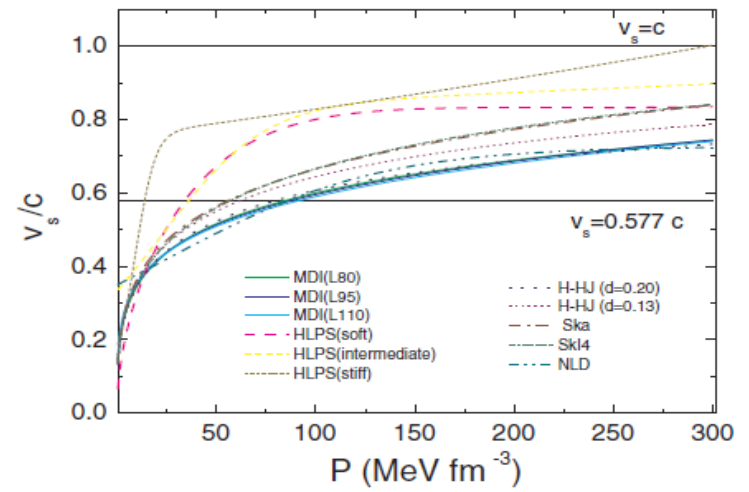


FIG. 2. The speed of sound dependence on the pressure for the EoSs used in the paper. The two specific upper bounds considered in the present work $v_s = c$ and $v_s = c/\sqrt{3} \simeq 0.577c$ are also indicated.

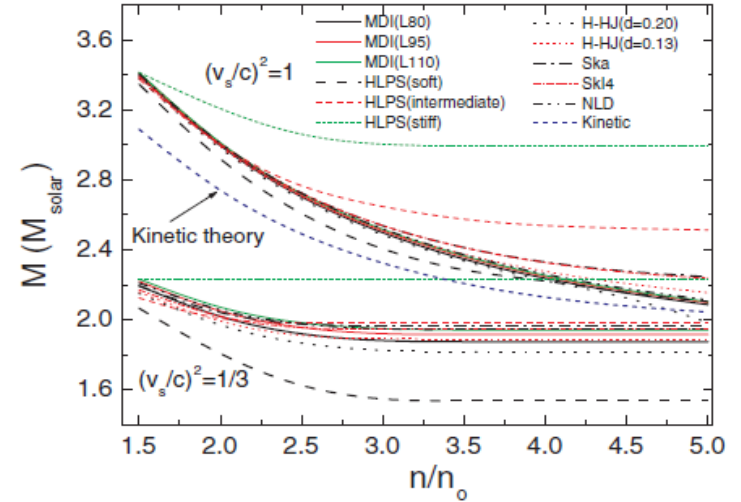
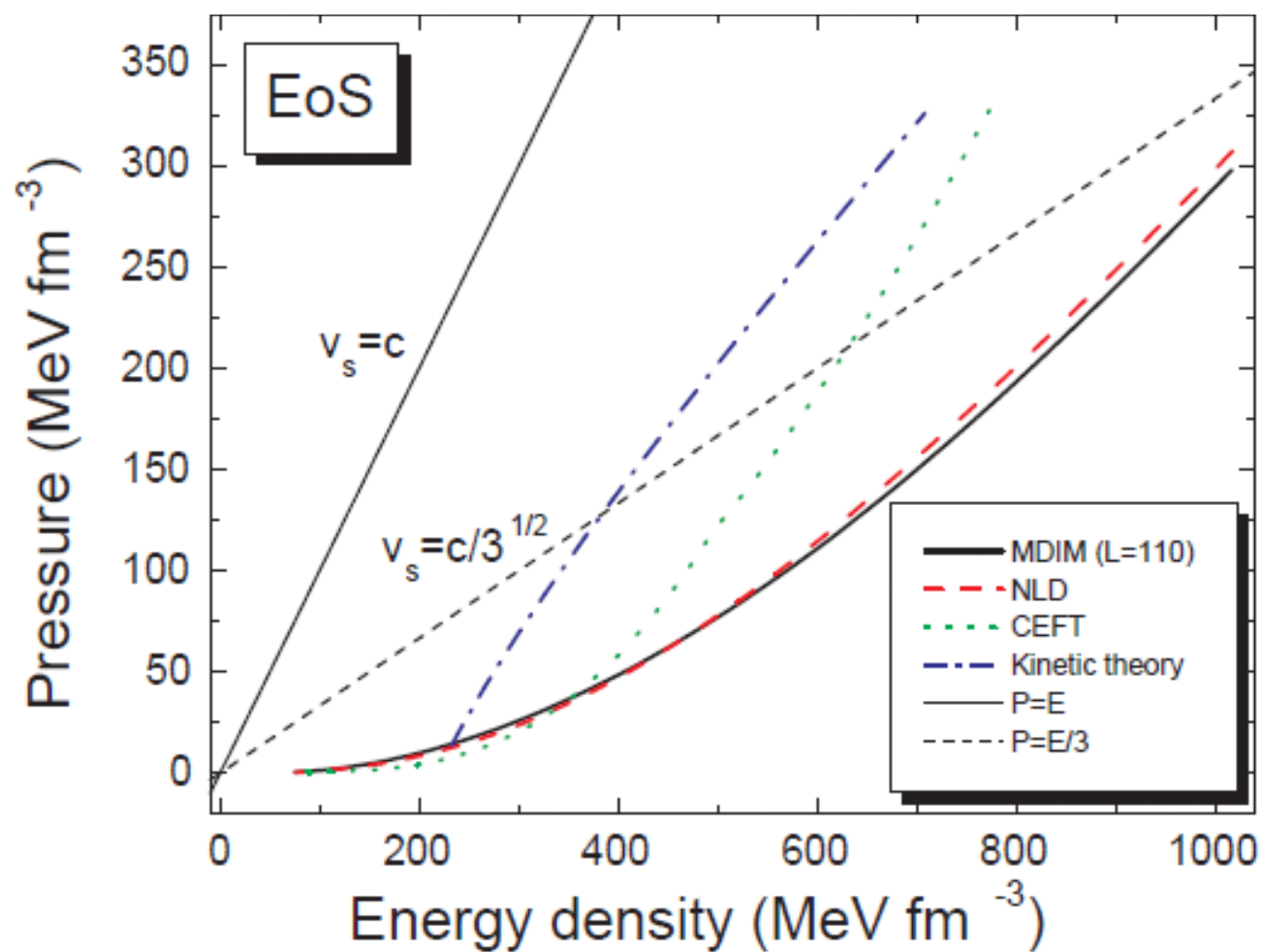


FIG. 4. The maximum mass of neutron stars as a function of the critical density n_0 for the two upper bounds for the speed of sound $v_s = c$ and $v_s = c/\sqrt{3}$. The case which corresponds to the upper bound for v_s , which is taken from the kinetic theory, is also indicated.



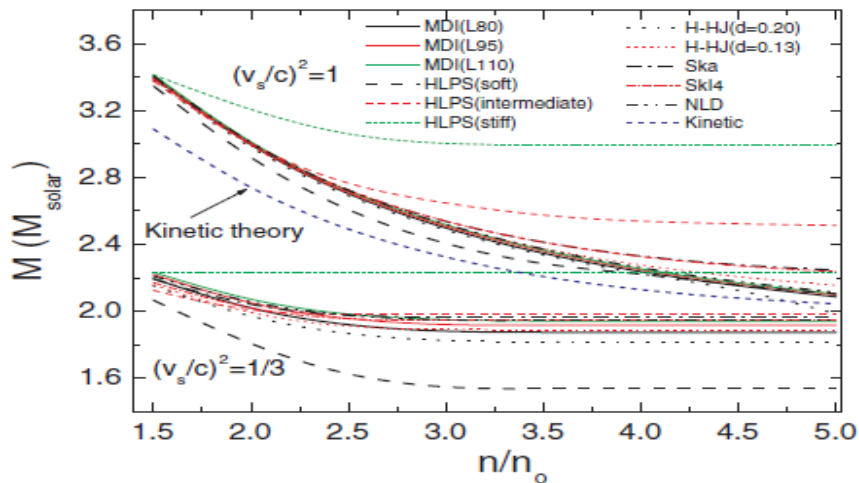


FIG. 4. The maximum mass of neutron stars as a function of the critical density n_0 for the two upper bounds for the speed of sound $v_s = c$ and $v_s = c/\sqrt{3}$. The case which corresponds to the upper bound for v_s , which is taken from the kinetic theory, is also indicated.

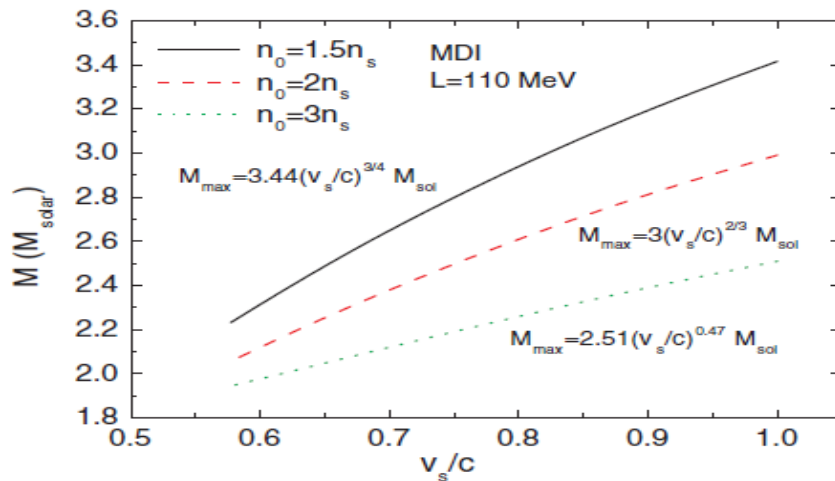


FIG. 5. The maximum mass as function of the upper bound of the speed of sound and for three different values of the critical density. The dependence is of the form $M_{\max} = a(v_s/c)^b M_{\odot}$. The values of the parameters a and b , for each case, have been selected by a least-squares fit method.

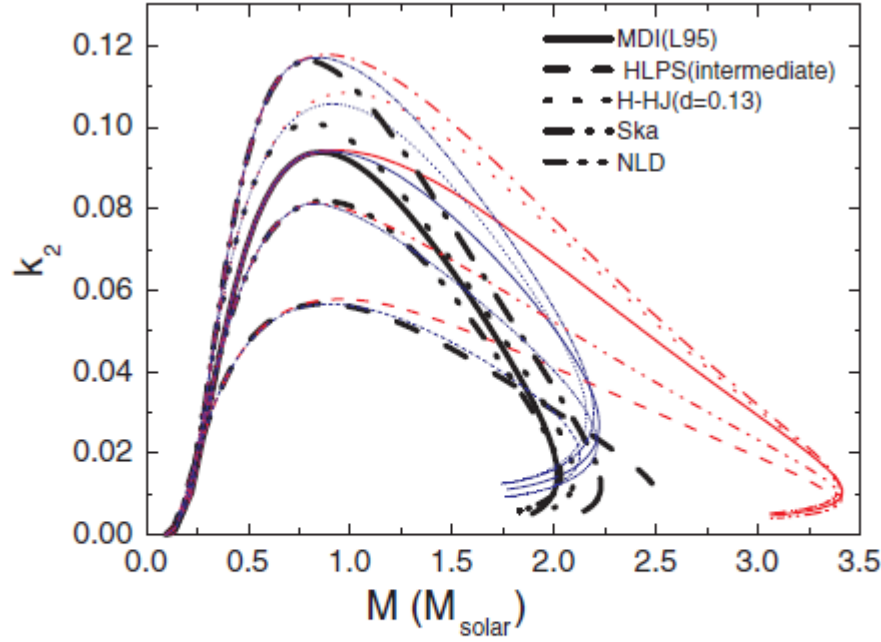


FIG. 6. The tidal Love number k_2 as a function of the mass for the five selected EoS's (EoS/normal case) in comparison with the corresponding maximum mass configuration results (EoS/minstiff and EoS/maxstiff cases). The notation is as in Fig. 3.

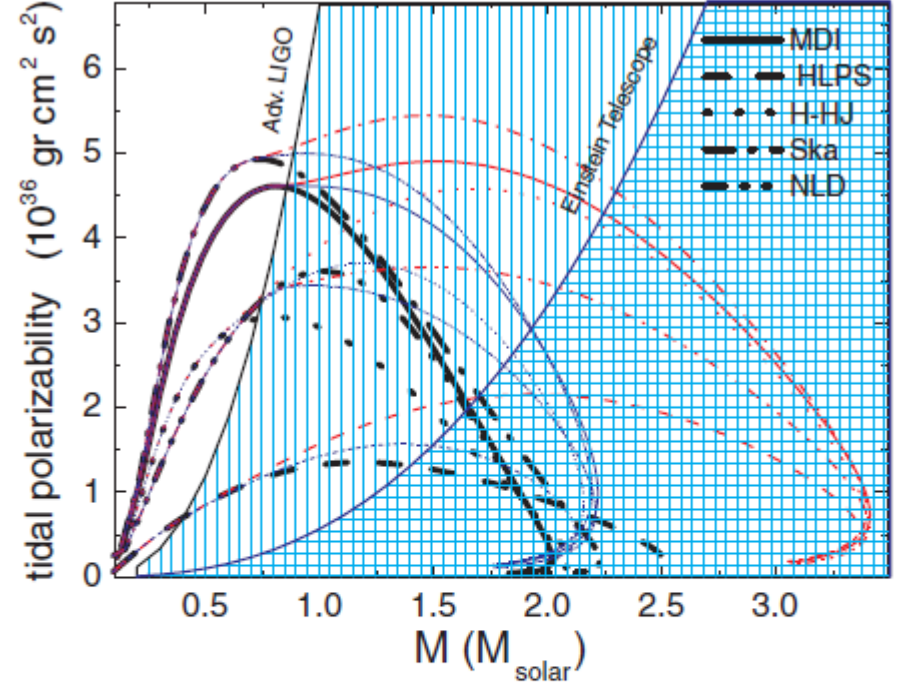


FIG. 7. The tidal polarizability λ of a single neutron star as a function of the mass for the five selected EoS's (EoS/normal case) in comparison with the corresponding maximum mass configurations results (EoS/minstiff and EoS/maxstiff cases). The notation is as in Fig. 3. The ability detection region of the Advanced LIGO is the unshaded region and the corresponding of the Einstein Telescope by the unshaded and light shaded region (see text for more details and also Ref. [57]).

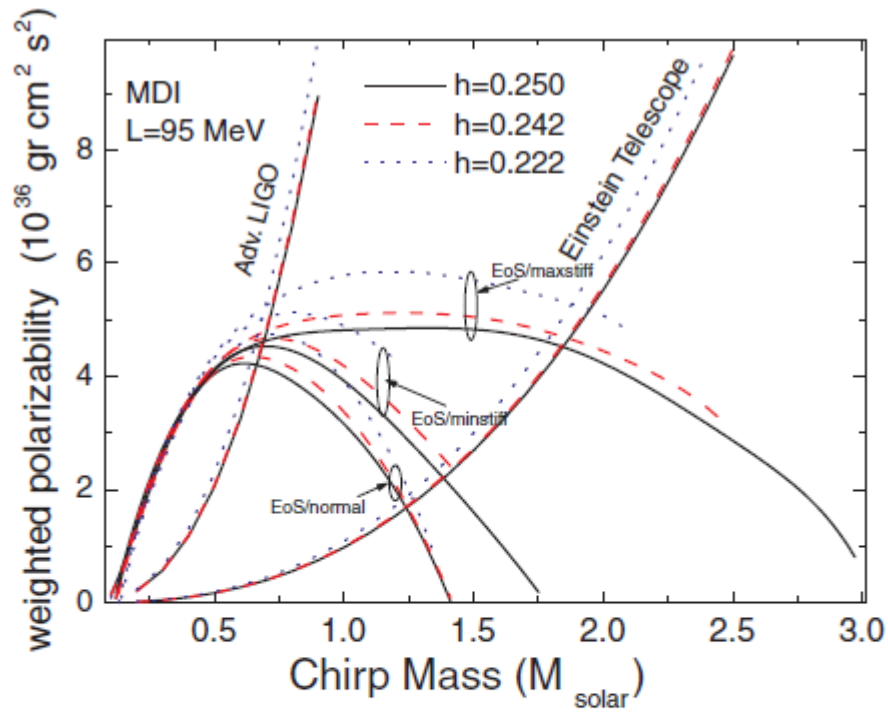


FIG. 8. The weighted tidal polarizability $\tilde{\lambda}$ as a function of the chirp mass \mathcal{M} for various values of the symmetric ratio η for the three considered cases (EoS/normal, EoS/minstiff, and EoS/max stiff) which correspond to the MDI (L95) EoS. The three values of the symmetric ratio (0.25, 0.242, 0.222) corresponds to the mass ratio m_2/m_1 (1, 0.7, 0.5) (see also Ref. [57] for comparison). The uncertainty $\Delta\tilde{\lambda}$ in the $\tilde{\lambda}$ measure of the Advanced LIGO and the corresponding of the Einstein Telescope are also indicated (for more details see text and also Ref. [57]).

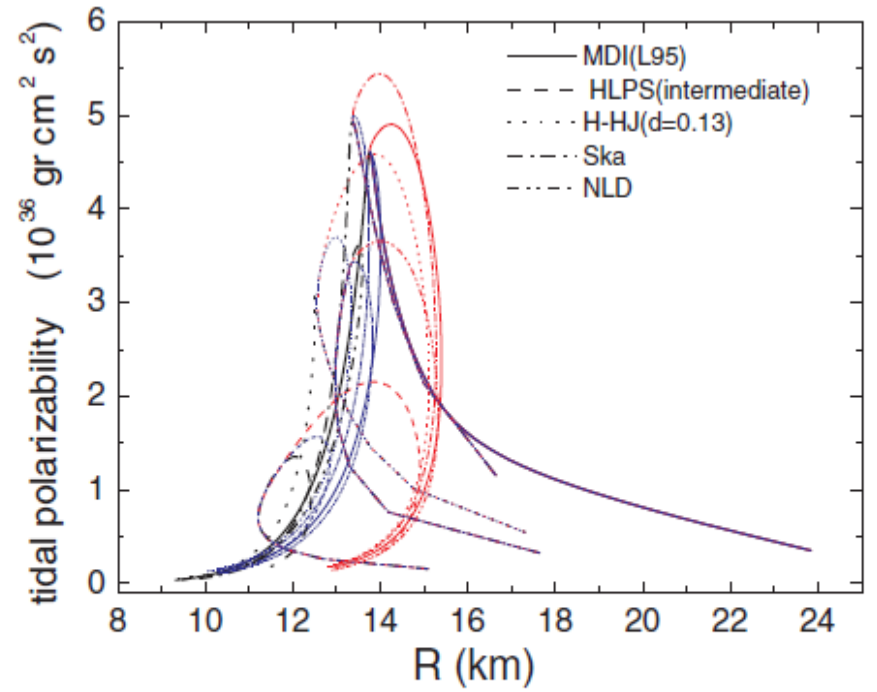


FIG. 9. The tidal polarizability λ as a function of the radius for the five selected EoS's in comparison with the corresponding maximum mass configuration results.

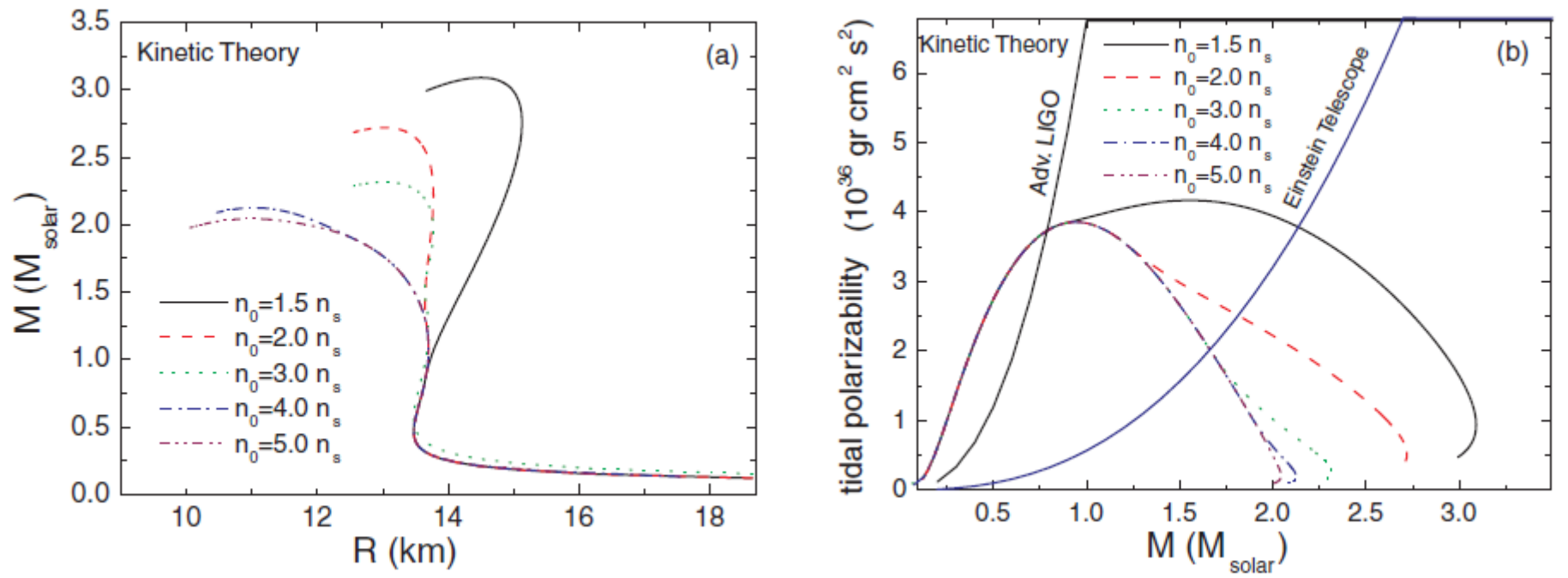


FIG. 10. (a) The mass-radius diagram which corresponds to the constraints for the relativistic kinetic theory in the v_s and for various values of the critical density n_0 (see text for more details), (b) The M - λ dependence from the kinetic theory in comparison with the observation abilities (see text for more details). The uncertainty $\Delta\lambda$ in the λ measure of the Advanced LIGO and the corresponding of the Einstein Telescope are also indicated (see also Fig. 7).

Conclusions-Outlook

- The knowledge of MNSM is important in order to identify the low mass black holes especially in binary systems
- The upper bound of the speed of sound is still an open problem in strongly interactive systems.
- The stiffness of the equation of state strongly constrained by the upper limit of the speed of sound. The upper limit $v_s=c$ is compatible with maximum mass up to 3 Msolar .
- However the limit $v_s=c/3^{1/2}$ is in contradiction with the recent measurements of neutron star with mass close to 2 Msolar.
- The relativistic kinetic theory predict M_{\max} close to the value 2.7 Msolar.
- The tidal polarizability is sensitive to the EoS and the relevant constraints introduced by the speed of sound
- We believe that the simultaneous measure of M and λ will help to better understand the stiffness limit of the equation of state.
- Observation with third-generation detectors will be able to definitely provide constraints for the stiffness of the EoS at high density and consequently to provide more information related with the upper bound of the speed of sound

General Perspectives

- The maximum and the minimum limit of neutron star mass related with the nuclear equation of state at supranuclear and subnuclear densities respectively
- Precise measurements of masses and radii for several individual neutron stars would pin down the equation of state without recourse to models
- The hadrons-quark phase transition at high densities.
- The link between the microphysics of transport, heat flow, superfluidity, viscosity, vortices tubes and the macro-modes in neutron star phenomenology
- Measuring the neutron star equation of state with gravitational waves observations
- Alternative theories (from general relativity) concerning mainly the strong-field regime